

Publication Year	2015
Acceptance in OA	2020-05-27T09:07:11Z
Title	Geometrical constraints on the origin of timing signals from black holes
Authors	Motta, Sara. E., CASELLA, Piergiorgio, Henze, M., Muñoz-Darias, T., Sanna, A., Fender, R., BELLONI, Tomaso Maria Melchiorre
Publisher's version (DOI)	10.1093/mnras/stu2579
Handle	http://hdl.handle.net/20.500.12386/25210
Journal	MONTHLY NOTICES OF THE ROYAL ASTRONOMICAL SOCIETY
Volume	447

Monthly Notices
of the
ROYAL ASTRONOMICAL SOCIETY

MNRAS **447,** 2059–2072 (2015) doi:10.1093/mnras/stu2579

Geometrical constraints on the origin of timing signals from black holes

S. E. Motta,[1⋆] P. Casella,[2] M. Henze,[1] T. Muñoz-Darias,[3] A. Sanna,[4] R. Fender[3] and T. Belloni[5]

[1]*ESAC, European Space Astronomy Centre, Villanueva de la Cañada, E-28692 Madrid, Spain*
[2]*INAF-Osservatorio Astronomico di Roma, Via Frascati 33, I-00040 Monteporzio Catone, Italy*
[3]*University of Oxford, Department of Physics, Astrophysics, Denys Wilkinson Building, Keble Road, Oxford OX1 3RH, UK*
[4]*Dipartimento di Fisica, Universitá degli Studi di Cagliari, SP Monserrato-Sestu km 0.7, I-09042 Monserrato, Italy*
[5]*INAF-Osservatorio Astronomico di Brera, Via E. Bianchi 46, I-23807 Merate, Italy*

Accepted 2014 December 4. Received 2014 November 24; in original form 2014 July 18

ABSTRACT

We present a systematic study of the orbital inclination effects on black hole transients fast time-variability properties. We have considered all the black hole binaries that have been densely monitored by the *Rossi X-ray Timing Explorer* satellite. We find that the amplitude of low-frequency quasi-periodic oscillations (QPOs) depends on the orbital inclination. type-C QPOs are stronger for nearly edge-on systems (high inclination), while type-B QPOs are stronger when the accretion disc is closer to face-on (low inclination). Our results also suggest that the noise associated with type-C QPOs is consistent with being stronger for low-inclination sources, while the noise associated with type-B QPOs seems inclination independent. These results are consistent with a geometric origin of the type-C QPOs – for instance arising from relativistic precession of the inner flow within a truncated disc – while the noise would correspond to intrinsic brightness variability from mass accretion rate fluctuations in the accretion flow. The opposite behaviour of type-B QPOs – stronger in low-inclinations sources – supports the hypothesis that type-B QPOs are related to the jet, the power of which is the most obvious measurable parameter expected to be stronger in nearly face-on sources.

Key words: binaries: close – stars: black holes – stars: jets – stars: low-mass – stars: oscillations – X-rays: binaries.

1 INTRODUCTION

Quasi-periodic oscillations (QPOs) were discovered several decades ago in the X-ray flux emitted from accreting black hole (BH) binaries and have been observed in many systems. In a Fourier power density spectrum (PDS), they take the form of relatively narrow peaks and appear together with different kinds of broad-band noise (e.g. Takizawa et al. 1997; Casella, Belloni & Stella 2005; Motta et al. 2012). It is now clear that QPOs are a common characteristic of accreting BHs and they have been observed also in neutron stars (NS) binaries (e.g. van der Klis 1989; Homan et al. 2002; Belloni et al. 2007), in cataclysmic variable (see e.g. Patterson, Robinson & Nather 1977) in the so-called *ultraluminous X-ray sources* (possibly hosting intermediate-mass BHs; e.g. Strohmayer & Mushotzky 2003) and even in active galactic nuclei (AGNs; e.g. Gierliński et al. 2008; Middleton & Done 2010).

Low-frequency QPOs (LFQPOs), with frequencies ranging from a few mHz to ∼20 Hz were first observed with *Ariel 6* in the BH binary (BHB) GX 339−4 (Motch et al. 1983) and observations with *Ginga* provided the first indications for the existence of multiple types of LFQPOs (see e.g. Miyamoto & Kitamoto 1991 and Takizawa et al. 1997). Three main types of LFQPOs, type-A, type-B and type-C,[1] originally identified in the PDS of XTE J1550−564 (see e.g. Wijnands, Homan & van der Klis 1999; Homan et al. 2001; Remillard et al. 2002; Casella et al. 2005; Motta et al. 2011) have been seen in several sources. These are distinct from the high-frequency QPOs, found at frequency up to ∼450 Hz, which we do not consider in this work (but see Belloni, Sanna & Méndez 2012, for a review).

The origin of LFQPOs is still unclear and there is no consensus about their physical nature, although their study provides a valuable way to explore accretion around accreting compact

⋆ E-mail: smotta@sciops.esa.int

[1] Type-C QPOs are by far the most common type of QPOs observed in BHBs. Their amplitude is usually large and they are characterized by a variable frequency ranging the 0.1–30-Hz interval. Type-B QPOs are less common than the type-C QPOs, they are usually observed along the transition from hard to soft in transient BHBs with frequencies around ∼6 Hz. Among LFQPOs, type-A QPOs are the least common of all. They usually appear in the soft states of transient BHBs as broad and weak peaks.

© 2015 The Authors
Published by Oxford University Press on behalf of the Royal Astronomical Society

Downloaded from https://academic.oup.com/mnras/article-abstract/447/2/2059/2593782 by tomaso.belloni@inaf.it on 11 May 2020

objects. Several models have been proposed to explain the origin and the evolution of LFQPO in X-ray binaries (XRBs). Some of them invoke the effects of general relativity (GR; e.g. Stella & Vietri 1999; Ingram, Done & Fragile 2009; Motta et al. 2014b), while others are based on different kinds of instabilities (e.g. Tagger & Pellat 1999; Titarchuk & Osherovich 1999; Lamb & Miller 2001). On the other hand, several doubts still surround the origin of type-B QPOs, for which no comprehensive model has been proposed. However, it has been speculated that type-B QPOs are associated with the strong relativistic jets that occurs in BHBs during specific state transitions (Fender, Homan & Belloni 2009; Miller-Jones et al. 2012).

It has been known for a long time that inclination strongly affects the observed properties of AGNs (see e.g. Antonucci 1993; Urry & Padovani 1995; Risaliti, Elvis & Nicastro 2002; Bianchi, Maiolino & Risaliti 2012). Over the last years, it has become increasingly clear that the same is true for Galactic accreting BHBs. Ponti et al. (2012) found strong evidences that the accretion disc winds observed in the radio quiet soft states of BHBs have an equatorial geometry with opening angles of a few degrees and therefore can only be observed in sources where the disc is inclined at a large angle i to the line of sight (*high-inclination sources*, as opposed to *low-inclination sources*, where the orbital plane is closer to perpendicular to the line of sight). More recently, the results by Muñoz-Darias et al. (2013) supported the hypothesis that the inclination modifies the q-shaped tracks that BHB in outburst display in a hardness–intensity diagram (HID; Homan et al. 2001), which can be at least partially explained by considering inclination-dependent relativistic effects on the accretion disc. Finally, Corral-Santana et al. (2013) have found that obscuration effects similar to those observed in AGN, can be relevant in very high inclination BHBs. However, Gallo, Fender & Pooley (2003) and Soleri & Fender (2011) noted that there is no evidence that the hard state radio luminosity is a function of inclination.

In this work, we use data collected by the *Rossi X-ray Timing Explorer* (*RXTE*)/Proportional Counter Array (PCA) satellite to analyse the effects of inclination on the fast time-variability properties of BHBs.

2 OBSERVATIONS AND DATA ANALYSIS

The main goal of this work is to perform a systematic study on the effect of the orbital inclination on the most common QPOs observed in BHs (i.e. type-C and type-B QPOs) and their associated noise.

To do so, we assume that there is no intrinsic difference between low-inclination and high-inclination systems. Therefore, any systematic difference observed between the QPO properties of systems viewed at different inclinations has to be mainly due to this parameter. We base our assumption on the fact that the outburst evolution and the macroscopic properties (e.g. orbital parameters; see Muñoz-Darias et al. 2013 where a similar source selection is performed) of these systems do not show any obvious difference.

2.1 The sample

For our analysis, we considered only the sources that have shown LFQPOs. We only investigate those that have been densely monitored by *RXTE*, in order to maximize the chances of observing high-inclination features (i.e. X-ray absorption dips or eclipses), if present. This is because accurate inclination measurements are not generally available for most of the sources (see Casares & Jonker 2014).[2] We therefore used the presence/absence of absorption dips as the main discriminant to separate high- and low-inclination sources (see also Appendix A and B). Note that transient BHBs usually have relatively short orbital periods (from a few days down to a few hours; see e.g. Casares & Jonker 2014), therefore absorption dips can appear quite often and it is in principle reasonably easy to detect them with a good observation coverage. This simplistic approach was applied in two previous works where it has been shown that the sources of both groups present, depending on the orbital inclination, different behaviours when looking at the spectral properties (i.e. colours and disc temperatures; Muñoz-Darias et al. 2013) and at the presence/absence of winds (Ponti et al. 2012).

Our sample includes the following 14 sources: Swift J1753.5−01, 4U 1543−47, XTE J1650−500, GX 339−4, XTE J1752−223, XTE J1817−330, 4U 1630−47, GRO J1655−40, H1743−322, MAXI J1659−15, XTE J1748−288, XTE J1550−564, XTE J1859+226, MAXI J1543−564 (see Table 1). XTE J1859+226 and MAXI J1543−564 have been treated separately because they cannot be unambiguously placed in either the high-inclination or the low-inclination group (see Appendix B). We refer to them as intermediate-inclination sources.

We excluded from this work XTE J1118+480, XTE J1652−453 and XTE J1720−318, GS 1354−64[3] because they did not display any significant QPO during the outbursts covered by *RXTE*. We also excluded GRS 1915+105 (see e.g. Fender & Belloni 2004; Soleri, Belloni & Casella 2008) and IGR J17091−3624 (e.g. Altamirano et al. 2011) because of their unusual outburst evolution, which is different to that of the other sources (i.e. they did not display a clear q-shaped HID).

The classification above results in a grouping where high and low inclination roughly mean inclination angle larger and smaller than $\sim$65°–70°, respectively. This value, however, must be taken with caution as the exact threshold for high inclination depends on the characteristic of each system, such as mass ratio between BH and companion star, orbital separation, dimension of the accretion disc and of the bulge that forms were the material from the companion star hits the accretion disc. This topic is addressed in detail in Appendix A.

2.2 Data analysis

We examined all the *RXTE* archival observations of the sources in our sample. For each observation, we computed power spectra from *RXTE*/PCA data using custom software under IDL[4] in the energy band 2–26 keV (absolute PCA channel 0 to 62). We used 128 s-long intervals and a Nyquist frequency of 1024 Hz. We averaged the PDS and subtracted the contribution due to Poissonian noise (see Zhang et al. 1995). The PDS were normalized according to Leahy, Elsner & Weisskopf (1983) and converted to square fractional rms (Belloni & Hasinger 1990).

We selected for our analysis only observations where a somewhat narrow (quality factor[5] $Q > 2$) low-frequency (< 50 Hz) feature was identifiable on top of flat-top or power-law shaped noise

[2] Note, however, that the accurate inclination measurements available for a few sources (see Table 1) mostly come from optical spectrophofometric observations (see Appendix B).

[3] Additionally, GS 1354−64 has been observed by *RXTE* only seven times.

[4] GHATS, http://www.brera.inaf.it/utenti/belloni/GHATS_Package/Home.html

[5] $Q = \nu_{\rm centroid}/{\rm FWHM}$, where $\nu_{\rm centroid}$ is the centroid frequency of the QPO fitted with a Lorentzian and FWHM its full width half-maximum.

Downloaded from https://academic.oup.com/mnras/article-abstract/447/2/2059/2593782 by tomaso.belloni@inaf.it on 11 May 2020

Table 1. List of BH transients and outbursts included in this work. In the column *comments* we report some information about the behaviour of the sources relevant to distinguish between high- and low-inclination systems. With *high-inclination evolution (High-IE)*, *intermediate-inclination evolution (Int.-IE)* and *low-inclination evolution (Low-IE)* we refer to high, intermediate and low disc temperatures, respectively, as reported in Muñoz-Darias et al. (2013). As discussed by these authors, the differences in the disc temperatures can be largely ascribed to the inclination of the disc to the line of sight. With the term *spikes*, we refer to flux spikes visible in both the light curve and HIDs of most high-inclination systems (see Muñoz-Darias et al. 2013). The term *winds* or *dipping* in the *comments* column indicate that equatorial winds or absorption dips, respectively, have been reported for that source.

System	Outburst	Inclination[e] (°)	Comments	Ref.	Type-A	Type-B	Type-C
Swift J1753.5−01	2005–2010	∼40–55	Failed outburst[d]	0			32
4U 1543−47	2002	20.7 ± 1.5	Low-IE;	1	2	3	11
XTE J1650−500	2001	> 47	Low-IE;	2		1	25
GX 339−4	2002, 2004, 2007, 2010	≥ 40[c]	Low-IE;	3	4	23	54
XTE J1752−223	2009	≤ 49[a]	Low-IE;	4		2	4
XTE J1817−330	2006		Low-IE;		2	9	2
XTE J1859+226	1999	≥ 60[b]	Int.-IE (spikes)	5	5	19	24
MAXI J1543−564	2011		Spikes;				5
XTE J1550−564	1998, 2000	74.7 ± 3.8	high-IE (spikes); dipping;	6, 7	1	18	48
4U1630−47	2002, 2003, 2004, 2005		high-IE (spikes); dipping; winds;	8, 9		6	19
GRO J1655−40	1996, 2005	70.2 ± 1	high-IE (spikes); dipping; winds;	8, 10		4	50
H1743−322	2003, 2004, 2008 (January and October), 2009, 2010 (January and August)	75 ± 3[a]	high-IE (spikes); dipping; winds;	11, 12, 13		42	108
MAXI J1659−152	2010		Spikes; dipping;	14		8	40
XTE J1748−288	1998		Spikes; dipping;				7

[a]Assuming that the radio jet is perpendicular to the accretion disc.
[b]Inclination ∼60° if accretion disc does not contribute to the optical luminosity in quiescence.
[c]The constrain is placed assuming that the mass of the BH should not be larger than 20 $M_{\odot}$.
[d]Failed outburst (see Soleri et al. 2013).
[e]Inclination measurements come either form the X-rays or from multiwavelength observations (moslty optical and radio).
References: (0) Neustroev et al. (2014); (1) Orosz et al. (2002); (2) Orosz et al. (2004); (3) Muñoz-Darias, Casares & Martínez-Pais (2008); (4) Miller-Jones et al. (2011); (5) Corral-Santana et al. (2011); (6) Orosz et al. (2011); (7) Homan et al. (2001); (8) Kuulkers et al. (1998); (9) Tomsick, Lapshov & Kaaret (1998); (10) Greene, Bailyn & Orosz (2001); (11) Corbel et al. (2005); (12) Steiner et al. (2012a); (13) Homan et al. (2005a) and (14) Kuulkers et al. (2013).

Table 2. QPO, noise and total rms from all the observations on the sources of our sample. We separated type-C and type-B QPOs and high- and low-inclination sources. The full table is available online only.

No.	ID	Frequency (Hz)	QPO rms (per cent)	Noise rms (per cent)	Total rms (per cent)
Type-C – low inclination (<70°)					
Swift J1753.5−01					
1	91094-01-01-00	$0.639^{+0.009}_{-0.009}$	$6.7^{+0.6}_{-0.6}$	$33.5^{+0.7}_{-0.6}$	$34.1^{+0.7}_{-0.6}$
2	91094-01-01-01	$0.823^{+0.006}_{-0.006}$	$10.5^{+0.6}_{-0.6}$	$30.7^{+1.2}_{-1.1}$	$32.5^{+1.1}_{-1.0}$
3	91094-01-01-02	$0.842^{+0.005}_{-0.005}$	$9.6^{+0.5}_{-0.5}$	$31.9^{+1.6}_{-1.5}$	$33.3^{+1.5}_{-1.4}$
4	91094-01-01-03	$0.824^{+0.005}_{-0.005}$	$12.3^{+0.5}_{-0.5}$	$30.2^{+3.8}_{-3.3}$	$32.6^{+3.6}_{-3.1}$
5	91094-01-01-04	$0.832^{+0.006}_{-0.006}$	$14.6^{+0.8}_{-0.7}$	$29.0^{+1.4}_{-1.3}$	$32.5^{+1.3}_{-1.2}$
...					

components in the PDS. PDS fitting was carried out with the XSPEC package by using a one-to-one energy–frequency conversion and a unit response. Following Belloni, Psaltis & van der Klis (2002), we fitted the noise components with a number of broad Lorentzian shapes. LFQPOs are well described by a variable number of narrow Lorentzians depending on the presence of harmonic peaks. When more than one peak was present, we identified the fundamental based on the QPO evolution along the outburst. Based on the results of the fitting, we excluded from the analysis non-significantly detected features (significance[6] $\leq 3\sigma$). We measured the rms as the square root of the integral over all the available frequencies of each component in the fit to the PDS. This means that the rms values we reported are measured between 1/128 Hz and 1024 Hz. For each PDS, we measured the fractional rms of each component of the spectrum (i.e. each Lorentzian used to fit the spectrum). Whenever a QPO is formed by more than one harmonic peak, we measured the rms of the QPO adding in quadrature the rms of the harmonic peaks. The rms of the noise comes from all the remaining components. The total rms is measured adding in quadrature the rms of all the components of the PDS. We report in Table 2 the rms of the QPO, the rms of the noise and the total rms for each observation.

We classified the LFQPOs following the method outlined by Motta et al. (2012) (based on Casella et al. 2005), dividing them into type-A, type-B and type-C QPOs. We collected a total of

[6] The significance of QPOs is given as the ratio of the integral of the power of the Lorentzian used to fit the QPO divided by the negative 1σ error on the integral of the power.

Downloaded from https://academic.oup.com/mnras/article-abstract/447/2/2059/2593782 by tomaso.belloni@inaf.it on 11 May 2020

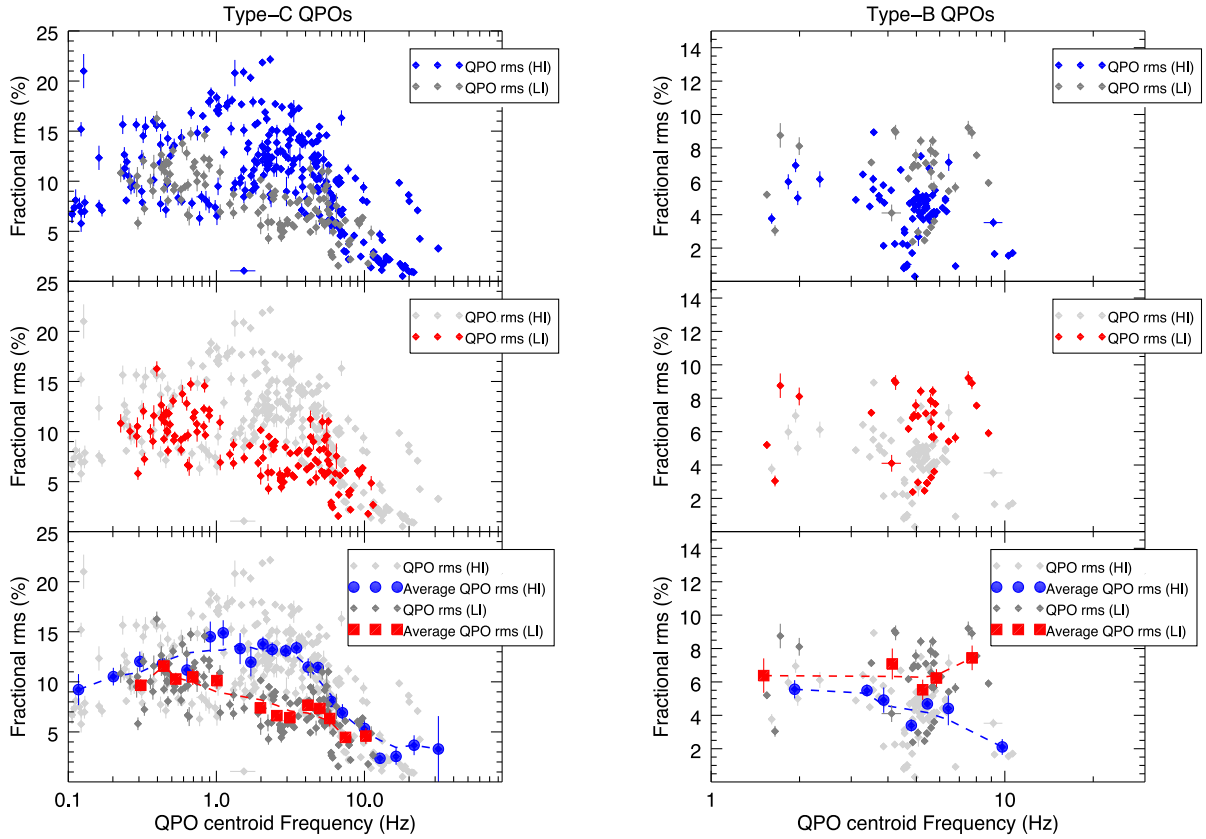

Figure 1. QPO rms as a function of the QPO centroid frequency for type-C QPOs (left figures) and type-B QPOs (right figures). For each figure, we plot as follows. In the top panel, we show data from high-inclination (HI) sources (blue) and from low-inclination (LI) sources (dark grey). In the middle panel, we plot the data from low-inclination sources (red) and from high-inclination sources (light grey). In the bottom panel light grey and dark grey points are the same as in the top and middle panel, the blue circles correspond to QPO detected in high-inclination sources, the red squares correspond to QPOs detected in low-inclination sources. The red squares and blue circles are 'average' points and have been obtained by applying a logarithmic rebin in frequency to the grey points. The dashed blue and red lines are smooth fits to the blue and red points, respectively, for visualizing. Here, we did not separate the sources, but we only distinguish between high- and low-inclination ones. Note that the axes are scaled differently for type-C and -B QPOs.

429 type-C QPOs, 135 type-B QPOs and 14 type-A QPOs (two from 4U 1543−47, two from XTE J1550−564, two from XTE J1817−330, four from XTE J1859+226 and four from GX 339−4). Due to the very low number of detections, we decided to exclude type-A QPOs from this work. In order to differentiate between the rms of the type-B/C QPO, the rms of the noise associated with a type-B/C QPO and the total rms of a PDS where we detected a type-B/C QPO, we will refer to type-B/C QPO rms, type-B/C noise rms and type-B/C total rms, respectively.

3 RESULTS

After classifying QPOs, we plotted the QPO rms and the noise rms as a function of the QPO centroid frequency, dividing the sources in high inclination and low inclination: we do not separate the different sources in order to give a better idea of the data general trend. The results are shown in Figs 1 and 2. Blue and red points always correspond to high-inclination and low-inclination sources, respectively. For clarity's sake, in each figure we display the data in the following way: in the top panel we show the data for high inclination sources in blue and the data from low-inclination sources in dark grey. In the middle panel, we show the data from low-inclination sources in red and the data from high-inclination sources in light grey. In the bottom panel, the light and dark grey dots are the same as in the top and middle panes, while the blue circles and red squares are 'average' points, obtained applying a logarithmic rebin in frequency to the grey points. The blues circles and the red squares represent data from high- and low-inclination sources, respectively.

In Fig. 3, we compare the distributions of rms for type-C and and type-B QPOs. In Fig. 4 we do the same, but this time we consider the noise associated with type-C and type-B QPOs. In Fig. 5, we compare the distributions of QPO centroid frequency for type-C and type-B QPOs. The plots in Figs from 3 to 5 show the histograms and the corresponding empirical cumulative distribution functions (ECDF). Blue represents high inclination, red low inclination and an overlap of the two colours in a histogram is indicated by mixing them into purple. As in the previous plots, we do not separate the different sources.

3.1 Statistical analysis

From Fig. 1, it is clear that at least the type-B and type-C QPO rms is different in high- and low-inclination sources in a quite large frequency range. To test the significance of these differences we carried out a two-sample Wilcoxon hypothesis test (*U*-test, also known as Mann–Whitney test; Mann & Whitney 1947). This is a non-parametric rank sum test designed to check for a difference in location shift. The idea is similar to testing the significance of the difference between two sample means in the popular Student's

Downloaded from https://academic.oup.com/mnras/article-abstract/447/2/2059/2593782 by tomaso.belloni@inaf.it on 11 May 2020

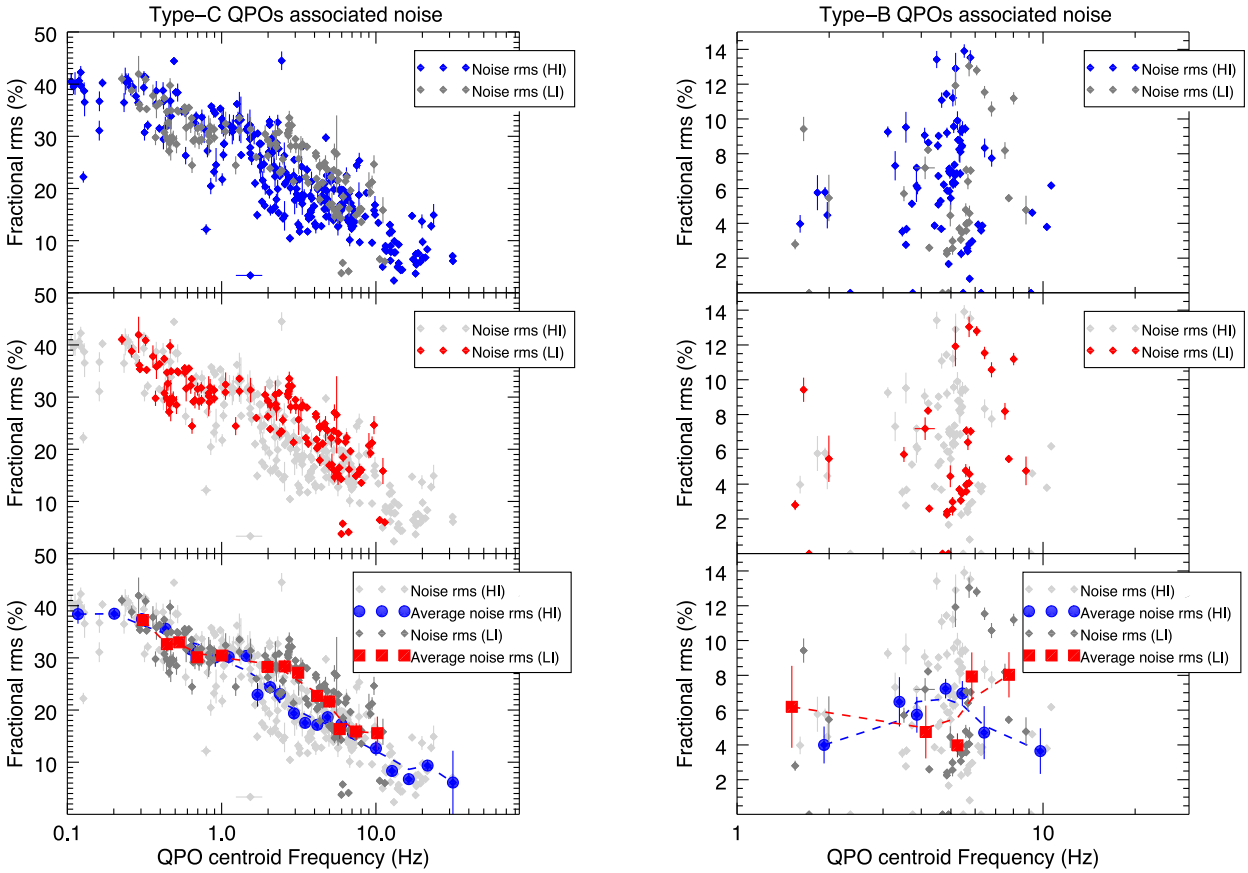

Figure 2. rms of the noise associated with the QPOs in Fig. 1 as a function of the QPO centroid frequency. Colour code is the same for Fig. 1. The average points have been produced as described in Fig. 1.

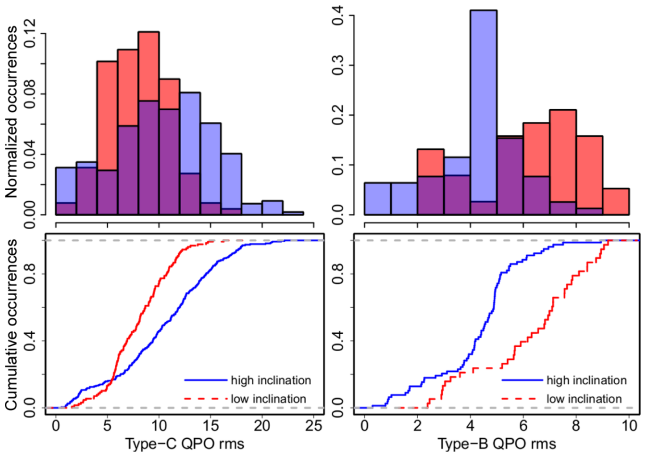

Figure 3. Type-B and type-C QPO rms distributions and correspondent ECDF. The distributions are different with high significance. Histograms are normalized to unit area.

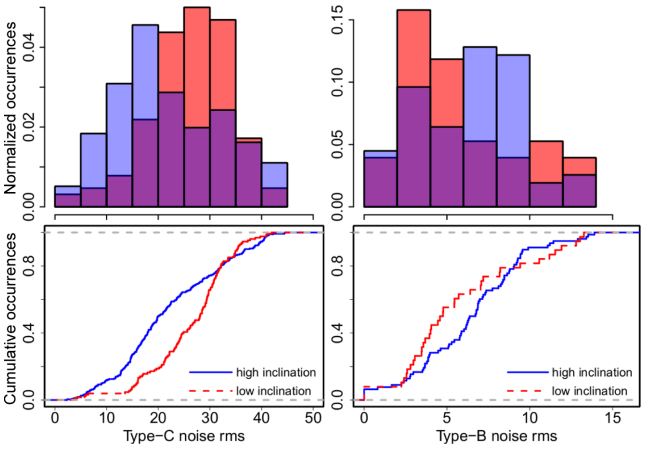

Figure 4. Type-B and type-C QPO associated noise rms distributions and correspondent ECDF. There is a significant difference for the type-C QPO noise distributions of about 4σ-equivalent confidence level. Histograms are normalized to unit area.

t-test. However, in our case many of the measured distributions are clearly not normal and therefore the *t*-test cannot be used. The only assumption of the *U*-test is that the shape of the two distributions is approximately similar. This is fulfilled here.

For the distributions in Fig. 3, where the similarity of shape might be doubted, we also performed a Kolmogorov–Smirnov test (KS-test), a different non-parametric test, which does not have this limitation. However, in order to interpret easily the results of the KS-test, the two ECDF should not intersect, a requirement that is clearly not fulfilled in the majority of cases in Figs 3–5. Therefore, we based our statistical inference primarily on the *U*-test. This analysis was performed within the R software environment (R Development Core Team 2011).

In Table 3, we summarize the results of the *U*-test for the high- and low-inclination ECDF in Figs 3–5. If the plots suggested an obvious difference between two ECDF we used a one-sided test, i.e.

Downloaded from https://academic.oup.com/mnras/article-abstract/447/2/2059/2593782 by tomaso.belloni@inaf.it on 11 May 2020

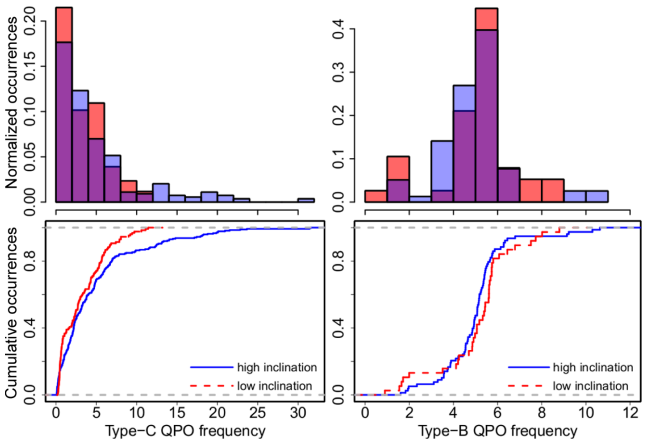

Figure 5. Type-B and type-C QPO frequency distributions for high- and low-inclination sources. The high- and low-inclination distribution for both type-C and type-B QPOs are broadly comparable. Histograms are normalized to unit area.

Table 3. Results of the statistical tests performed on the parameter distributions for the type-C, type-B QPOs and their associated noise. In the 'significance' column, we indicate whether the distributions we compare in each line are significantly different. S: distributions are significantly different (p-value < 0.01), MS: distributions are marginally different ($0.01 \leq p$-value ≤ 0.05), NS: distributions are not significantly different (p-value > 0.05).

Low versus high inclination	p-value	Significance
Type-C QPOs rms	3.421×10^{-8} (U-test)[a]	S
	8.482×10^{-9} (KS-test)	S
Type-B QPOs rms	1.047×10^{-6} (U-test)[a]	S
	5.857×10^{-8} (KS-test)	S
Type-C QPOs noise rms	1.108×10^{-5} (U-test)[b]	S
Type-B QPOs noise rms	0.1686 (U-test)[b]	NS
Type-C QPOs frequency	0.044 (U-test)[b]	MS
Type-B QPOs frequency	0.169 (U-test)[b]	NS

[a]and [b]indicate that a one-sided or a two-sided test, respectively, has been performed.

we tested whether there is a location shift into a specific direction (e.g. red is right of blue). For cases in which there was no clear visible difference, we tested for a non-zero location shift (i.e. two-sided test). Table 3 lists, for each test, the resulting p-value, which is the probability of obtaining a difference at least as large as observed if the underlying distributions were in fact identical.

3.2 Results from the tests

From the statistical tests described in Section 3.1, we find that the rms distributions of both type-C and type-B QPOs of high-inclination versus low-inclination sources are significantly different.

(i) Fig. 3: here, we compare the QPO rms distribution for type-C and type-B QPOs. For both QPOs the distributions of high- and low-inclination sources are very different. The type-C QPO rms appears to be, on average, higher for high-inclination sources, while the opposite is true for type-B QPOs that are stronger in low-inclination systems. In the case of type-C QPOs, the high- and low-inclination distributions are different mainly at intermediate frequencies (∼0.5–10 Hz), while they overlap at lower and higher frequencies (see Fig. 1). Also in the case of type-B QPOs, the distributions are significantly different and both a U and a KS-test[7] give similar results.

(ii) Fig. 4: this plot compares the rms of the noise associated with type-C and type-B QPOs. Again we separate type-B and -C QPOs. While the high- and low-inclination populations of type-B QPOs noise rms distributions are not significantly different, we detect a significant difference (about 4σ) in the case of type-C QPO noise, with the noise stronger for low-inclination sources (i.e. the noise does the opposite with respect to the QPOs). However, the difference is mainly due to the points between 1 and 8 Hz (see Fig. 2).

(iii) Fig. 5: this plot compares the QPO frequencies for type-C and type-B QPOs separately. The high- and low-inclination type-B QPO frequency distributions are broadly comparable, while the two type-C QPO frequency distributions are marginally different. This is probably due to the high-frequency tail in the high-inclination type-C QPO frequency distribution. This feature decreases the similarity between the distributions and the formal test should therefore be interpreted with care.

(iv) For completeness, we also compared the total rms distributions from the observations where a type-C or a type-B QPO was found. The distributions do not show significant differences. In the case of type-C QPOs, this is probably due to the fact that the QPO and the associated noise distributions show an opposite dependence on inclination that shifts the total rms distributions closer together. In the case of type-B QPOs, the total rms distribution is dominated by the noise (inclination independent) and the small difference between the type-B distributions is probably due to the presence of the (significantly different) QPO rms.

In order to study in greater detail the dependence of the amplitude (the rms) of the QPO on inclination, we produced two additional plots. The top- and bottom-left panels in Fig. 6 combine the ECDFs of the type-C QPO rms for all the individual sources. The right-hand panels show the same for type-B QPOs. High-inclination sources (top panels) are plotted in cyan, light blue, blue, purple, dark blue and black and low-inclination sources (bottom panels) are represented in yellow, orange, dark orange, red, pink and brown. In the case of type-C QPOs, there is some overlap, but high- and low-inclination sources can clearly be distinguished. The situation is somewhat less clear for the type-B QPO rms distributions, because of the dominance of GX 339−4, and maybe the fact that a couple of sources have so few measurements. XTE J1650−500 and XTE J1752−223 only displayed one and two type-B QPOs, respectively, therefore they do not provide any valid information.

Since GX 339−4 provides more type-B QPOs to the low-inclination group than any other source, we performed the tests described in Section 3.1 also excluding this source from the sample. For both the type-C and type-B noise distributions, as well as in the type-C QPOs distributions, we obtain similar results to what we report in Table 3 (low versus high inclination average QPO rms distributions without GX 339−4: p-value for type-C QPO is 2.033e−06). However, in the case of type-B QPOs we found that the difference in the high- and low-inclination distributions becomes only marginally significant (low versus high inclination average QPO rms distributions without GX 339−4: p-value for type-B QPO is 0.023), which could be mainly due to the reduction in sample size (number of data

[7] The KS-test is sensitive to location shifts as well as differences in the distribution shape.

Downloaded from https://academic.oup.com/mnras/article-abstract/447/2/2059/2593782 by tomaso.belloni@inaf.it on 11 May 2020

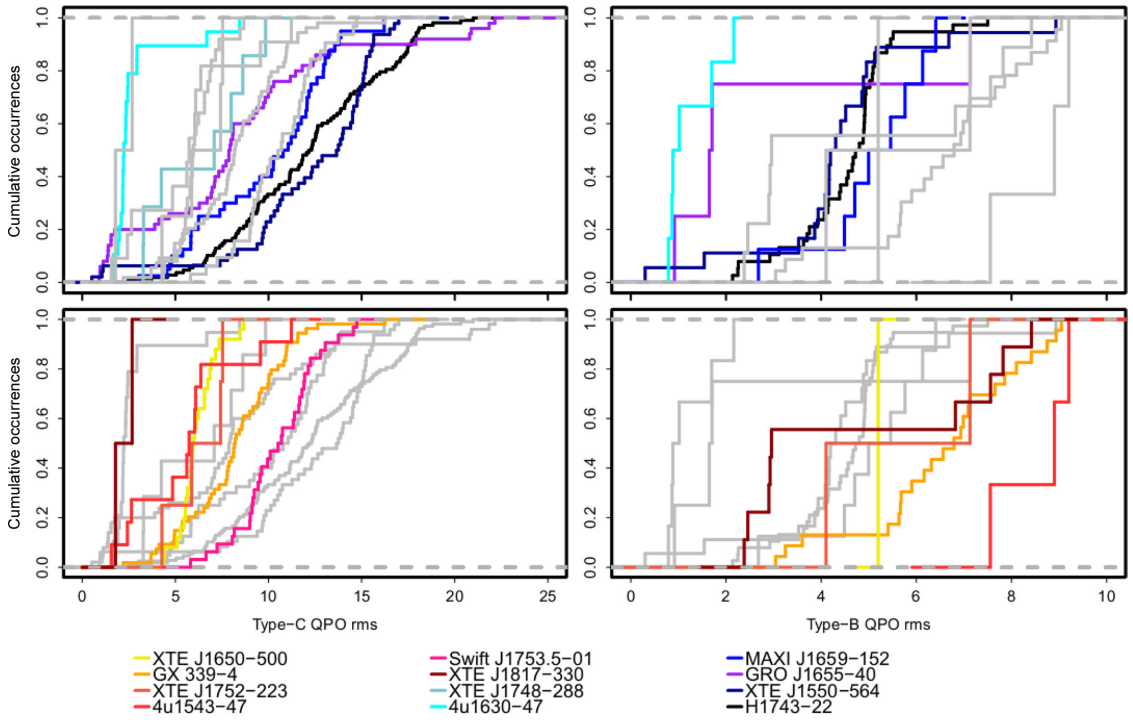

Figure 6. Cumulative QPO rms distributions (for type-C and B QPOs, left- and right-hand panels, respectively) for the individual sources of our sample. Different colours correspond to diffferent sources (see legend). To facilitate the comparison between the two population of sources, we first show the high-inclination sources in different colours and the low-inclination sources in grey (top panels) and then the low-inclination sources in colours and the high-inclination sources in grey.

points reduced from 38 to 15). Thus, it appears that the contribution from GX 339−4 dominates the low-inclination type-B QPO population. We also tested for significant differences between the QPO rms ECDF of GX 339−4 and the average low-inclination QPO rms distributions and we found no significant differences (GX 339−4 versus low-inclination average QPO rms distributions: p-value for type-C QPO is 0.397; p-value for type-B QPO is 0.46), suggesting that GX 339−4 shows no obvious deviation from the average low-inclination sources behaviour. Therefore, our results still hold despite the dominance of GX 339−4.

3.3 The case of XTE J1859+226 and MAXI J1543−564

As noted in Section 2.1, we could not unambiguously classify XTE J1859+226 and MAXI J1543−564 as high- or low-inclination systems. Therefore, we treat them separately here. In Fig. 7, we show a comparison between the QPO and noise rms ECDF for XTE J1859+226 and MAXI J1543−564 and the correspondent average ECDF for high- and low-inclination systems (shown in Fig. 3). We see that in the relevant cases (type-B/C QPO rms and type-C noise), despite some overlap with the average distributions, both systems qualitatively resemble the behaviour of high-inclination sources rather than low-inclination sources. We note, however, that we only have five type-C QPOs from MAXI J1543−564, therefore the statistics is fairly low in this case.

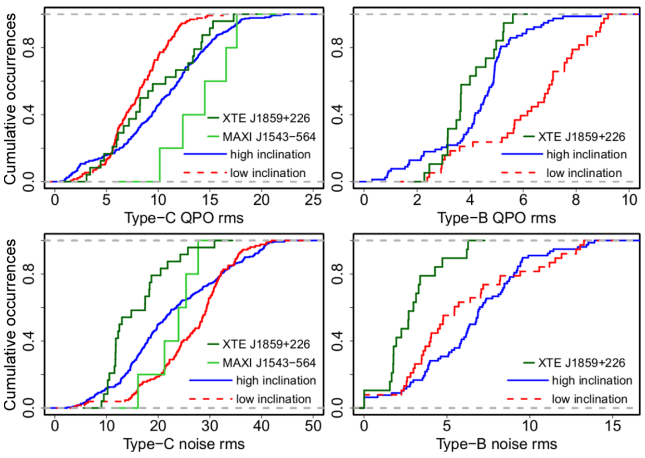

Figure 7. Cumulative QPO rms distributions (for type-C and B QPOs, top-left and top-right panels, respectively) and noise rms distributions (associated with type-C and -B QPOs, bottom-left and bottom-right panels, respectively) for XTE J1859+226 (dark green line) and MAXI J1543−564 (light green line). The red and blue line correspond to the average ECDF of low- and high-inclination sources, respectively, as it is shown in Fig. 3. Note that in the case of type-B QPOs, only XTE J1859+226 is shown since MAXI J1543−564 did not show any significant type-B QPOs during its outburst.

4 DISCUSSION

We used a large archival data set from the *RXTE* satellite to measure, with a 'population-statistics approach', the amplitude of the aperiodic variability (i.e. QPO amplitude and noise amplitude) in a number of BH X-ray transients. We collected a total of 564 QPOs: 128 type-C QPOs and 38 type-B QPOs from 6 low-inclination sources and 272 type-C QPOs and 78 type-B QPOs from 6 high-inclination sources. In addition, we collected 29 type-C QPOs and 19 type-B QPOs from intermediate-inclination sources.

Downloaded from https://academic.oup.com/mnras/article-abstract/447/2/2059/2593782 by tomaso.belloni@inaf.it on 11 May 2020

These are our main findings.

(i) We find a highly significant difference between the QPO rms distributions of high-inclination versus low-inclination sources. This is true for both type-C and type-B QPOs (even though the low-inclination type-B QPO population is somewhat dominated by GX 339−4). Our study confirms results obtained for a smaller sample of sources and observations by Schnittman, Homan & Miller (2006) for the case of type-C QPOs. The QPO amplitude correlates significantly with the inclination of the binary system: type-C QPOs are generally stronger in high-inclination sources (i.e. closer to edge on), while type-B QPOs are generally stronger in low-inclination sources (i.e. closer to face-on sources).

(ii) We find a significant difference in the noise distributions associated with type-C QPOs, while in the case of type-B QPOs the associated noise seems to be inclination independent. On average, the noise is consistent with being stronger for low-inclination sources (at least in a certain frequency range), at variance with the behaviour of QPOs. This constitute the first evidence that the broad-band noise associated with the QPOs shows a different behaviour with respect to the QPO themselves and, for this reason, could have a separate origin.

(iii) Comparing these results with the properties of XTE J1859+226 and MAXI J1543−564, we conclude that the inclination of these sources is consistent with being intermediate to high rather than low inclination, in line with what the properties listed in Table 1 suggested. Of course, accurate inclination measurements for both sources are needed to confirm this result.

Recently, with a grouping very similar to what we used, but through a different method, Heil, Uttley & Klein-Wolt (2014) found the same inclination dependence in the amplitude of type-C QPOs that we have found. Heil et al. (2014) also reported that the broad-band noise associated with type-C QPOs is inclination independent. However, since the comparison between high- and low-inclination sources performed by these authors is qualitative, their results are still broadly consistent with ours.

4.1 Caveats

4.1.1 The sample

Our sample of sources is quite small and tests on a different, independent sample of sources are needed to confirm our findings. Furthermore, in this work we focused only on the general differences in the QPOs and noise distributions, without investigating the details of the distributions themselves. However, the different dependence of the QPO rms on the orbital inclination already suggest that type-B and type-C QPOs are intrinsically different and could come from two well-defined geometrical regions. Most likely, they are the effect of different physical processes and/or the result of different geometrical configuration/physical properties (e.g. change in plasma temperature, ionization state, viscosity or optical depth) of the accreting material in the region where they are produced. This is supported by the results obtained by Motta et al. (2012) who discovered simultaneous type-C and type-B QPO in the data of the BHB GRO J1655−40. This result essentially ruled out the possibility that type-B QPOs could arise from the same physical phenomenon originating type-C QPOs – regardless of what this phenomenon is – supporting what was already suggested by Motta et al. (2011) based on the dependence of the different kind of QPOs on the hard emission.

4.1.2 Source classification and grouping

Since the inclination measurements are often not precise and affected by large uncertainties, our source classification mostly relies on the assumption that absorption dips are a strong indication of high orbital inclination. Even though this association is commonly adopted (see Appendix B), it represents a critical caveat for our results, as any new observation showing absorption dips might turn a low-inclination source into a high-inclination one (while it practically impossible for a high-inclination source to turn into a low-inclination one). Our choice of considering only well-monitored sources is intended to minimize the possible missing of a high-inclination feature. Even so, the misclassification of one or more sources is still possible as it is known that absorption dips can disappear during an outburst (see e.g. Smale & Wachter 1999; Kuulkers et al. 2013) – making their detection harder – or can be detected only after being well sampled by years of X-ray observations, as it happened in the case of H1743−322 (Homan et al. 2005a; see also D'Aì et al. 2014). In order to investigate the effects of such misclassification, we performed again the *U*-tests described in Section 3.1 on the high- and low-inclination distributions, but this time moving, one by one, the sources of the low-inclination group to the high-inclination group. We see that, predictably, the significance of the difference between the high- and low-inclination distributions tends to decrease when moving a low-inclination source to the high-inclination group. However, the difference remains always significant (p-value always < 0.001), with the exception of GX 339−4 in the case of the type-B QPOs rms distributions (p-value $= 0.082$). This is probably mainly due to the fact that GX 339−4, as we already discussed in Section 3.2, dominates (without biasing it) the low-inclination type-B QPOs rms distribution. We note, however, that GX 339−4[8] is the best monitored BHB of our sample and therefore it is also the least likely source to be misclassified.

Additionally, we see a considerable scatter within the QPO rms distributions of the high- and low-inclination groups (see Fig. 3). While the average difference between the two groups is highly significant, there is also an overlap of the individual source ECDFs. However, in Fig. 3 we clearly see that there are strong differences between the individual sources and that the QPO rms distributions cannot be considered similar. Evidently, it is in principle possible to group the sources differently from our categorization based on inclination. To test the goodness of our grouping, we randomly divided the twelve sources of our sample into two groups of six and used the same statistical test as above to compute the significance of the difference between the QPO rms distributions. For 10^6 of these random samplings, we found that in about 5 per cent of all cases the result is at least as significant as the one reported in Table 3 (after correcting for the large number of comparisons made). This is in agreement with the scatter visible in Fig. 3. Nonetheless, unlike all those random groupings, our initial classification was made a priori based on physical arguments. Therefore, its statistical significance conveys a physically meaningful result.

4.1.3 Inner–outer disc misalignment

It has been recently suggested (see Veledina, Poutanen & Ingram 2013) that a misalignment between orbital spin and BH spin (presumably aligned with the jet axis) might significantly influence the

[8] GX 339−4 has been observed with *RXTE* 1426 times over a time span of about 15 yr.

Downloaded from https://academic.oup.com/mnras/article-abstract/447/2/2059/2593782 by tomaso.belloni@inaf.it on 11 May 2020

rms amplitude of type-C QPOs in BHBs. In this context, the relevant angle for the precession is the angle between the BH spin and the line of sight, therefore a misalignment between spin and orbital plane (not considered here, as we use the angle between the line of sight and the orbital spin) could in principle largely affect the QPO amplitude. It is also worth noticing that the outer disc inclination and the inner disc inclination might differ from one another as the inner disc can be strongly affected by the BH spin, i.e. the inner disc might tend to align with the plane normal to the BH spin, while the outer disc tends to stay aligned with the orbital plane. The difficulty in estimating the BH spin/orbital spin misalignment constitutes an additional source of uncertainty and, together with the fact that most inclination measurements are poorly constrained, (especially in the case of nearly face-on sources, see Appendix B) prevents us from studying the details of the effects of inclination on the ECDFs.

4.2 About the origin of LFQPOs

The existing models that attempt to explain the origin of LFQPOs are generally based on two different mechanisms: instabilities and geometrical effects. In the latter case, the physical process typically invoked is precession.

Titarchuk & Fiorito (2004) proposed the so-called *transition layer model*, where type-C QPOs are the result of viscous magnetoacoustic oscillations of a spherical bounded transition layer, formed by matter from the accretion disc adjusting to the sub-Keplerian boundary conditions near the central compact object. This mechanism would not produce inclination-dependent QPOs and is, therefore, unable to explain our results.

Cabanac et al. (2010) proposed a model to explain simultaneously type-C QPOs and the associated broad-band noise. Magnetoacoustic waves propagating within the corona makes it oscillate, causing a modulation in the efficiency of the Comptonization process on the embedded photons. This should produce both the type-C QPOs (thanks to a resonance effect) and the noise that comes with them. This model predicts that both type-C QPOs and their associated noise would be inclination independent. Therefore, also the predictions of this model do not match the observed properties of the LFQPOs reported here.

Tagger & Pellat (1999) proposed a model based on the *accretion ejection instability* (AEI), according to which a spiral density wave in the disc, driven by magnetic stresses, becomes unstable by exchanging angular momentum with a Rossby vortex. This instability forms low azimuthal wavenumbers, standing spiral patterns which would be the origin of LFQPOs. Varnière & Tagger (2002) and Varnière, Tagger & Rodriguez (2012) suggested that all the tree types of QPOs (A, B and C) can be produced through the AEI in three different regimes: non-relativistic (type-C), relativistic [type-A, where the AEI coexist with the Rossby Wave Instability (RWI); (see Tagger & Pellat 1999) and during the transition between the two regimes. Varnière & Blackman (2005) investigated the impact of a clean spiral density wave on the emission from an accreting BH and found that the rms of type-C QPOs is expected to be higher when the disc is close to edge on (Varnière & Blackman 2005), therefore the AEI model succeeds in partly reproduce our findings. However, as the effects of the interplay of the RWI and the AEI must be taken into account, further investigation is needed to fully understand the predicted behaviour of type-B and type-A QPOs, as well of their associated noise (Varnière, private communication).

In summary, all the models based on instabilities fail in fully explaining the properties of the QPOs and of the noise. Therefore, we are left only with the models involving geometrical effects. The maximum radius at which an $\sim$ Hz modulation can be produced in a 10-$M_{\odot}$ BH would come from orbital motion at $>100R_g$ from the BH. Hence, in principle, type-C QPOs could be the result of modulation/occasional obscuration of the emission from the inner hot flow operated by structures in the disc (e.g. clumps in the accretion flow). However, in this case, a mechanism producing both obscuring structures – that would need to be unrealistically vertically extended to be able to partially obscure the emission from the inner flow – and a mainly equatorial emission from the inner flow is necessary to explain what we observed. Furthermore, Motta et al. (2014a,b) have shown that the Lense–Thirring mechanism successfully explain the evolution of type-C QPOs (and other timing features) in two BHBs (GRO J1655−40 and XTE J1550−564).

Ingram et al. (2009) proposed a model based on the relativistic precession as predicted by GR that attempts to explain type-C QPOs and their associated noise. This model requires a cool optically thick, geometrically thin accretion disc (Shakura & Sunyaev 1973) truncated at some radius, filled by a hot, geometrically thick accretion flow. This geometry is known as *truncated disc model* (Esin, McClintock & Narayan 1997; Poutanen, Krolik & Ryde 1997). In this framework, type-C QPOs arise from the Lense–Thirring precession of a radially extended section of the hot inner flow that modulates the X-ray flux through a combination of self-occultation, projected area and relativistic effects that become stronger with inclination (see Ingram et al. 2009). The broad-band noise associated with type-C QPOs, instead, would arise from variations in mass accretion rate from the outer regions of the accretion flow that propagate towards the central compact object, modulating the variations from the inner regions and, consequently, modulating also the radiation in an inclination-independent manner (see Ingram & van der Klis 2013). The predictions of this model match our findings if the anisotropy of the hot-flow emission is considered. Veledina et al. (2013) simulated the X-ray and optical emission predicted by this model for variable source inclination angles, taking into account also the possible relativistic effects on the accretion flow. From fig. 3 in Veledina et al. (2013), we infer that the angular dependence of the coronal emission varies with the distance from the BH. In particular, X-ray emission from the outer regions of the hot-flow (tens to hundreds gravitational radii) is more visible in low-inclination sources, while the opposite is true for the inner regions (3–5 gravitational radii), whose emission is more visible in high-inclination sources. Therefore, low-inclination sources should have a softer coronal emission than high-inclination sources. The broad-band noise is also known to have a soft spectrum, at least in the hard states (Gierliński & Zdziarski 2005). Although little can be said about the intrinsic energy dependence of the noise in the intermediate states (because of the soft emission from the disc) it is reasonable to assume that the noise itself does not change much its properties from the hard to the intermediate state, thus remaining soft (i.e. coming predominantly from the outer regions of the hot flow). This implies that the noise associated with type-C QPOs is expected to be stronger in face on sources, as we do observe in our data (at least when the QPO is found in a certain frequency range). In conclusion, the predictions of the model proposed by Ingram et al. (2009), Ingram & Done (2011), Ingram & Done (2012) and Ingram & van der Klis (2013) are consistent with the observed properties of both type-C QPOs and noise.

Type-B QPOs show an opposite behaviour to type-Cs, i.e. their amplitude is larger for low-inclination sources. Only the model by Tagger & Pellat (1999) attempts to explain the origin of type-B QPOs; however, our findings points to an intrinsic difference

Downloaded from https://academic.oup.com/mnras/article-abstract/447/2/2059/2593782 by tomaso.belloni@inaf.it on 11 May 2020

between type-C and type-B QPOs, which are still not fully explained by their model.

Type-B QPOs have been tentatively associated with the relativistic ejections usually observed along the hard-to-soft transitions in transient BHBs (Fender, Belloni & Gallo 2004), even though a clear cause-effect relation between the two phenomena has not been identified (Fender et al. 2009; Miller-Jones et al. 2012). There are two main ways in which the observed dependence on inclination of type-B QPOs could be produced, assuming that the type-B QPOs come from the jet: (i) a lack of obscuration when the observer is able to look directly into the jet; (ii) relativistic aberration due to the jet flow. In case (i) the oscillator responsible for the production of type-B QPOs needs not be physically associated with the relativistic outflow, while in case (ii) it would actually be part of the jet. However, in case (i) we would expect abrupt changes in the amplitude of the type-B QPO (see Nespoli et al. 2003), while more continuous changes would be expected in case (ii). In any case, the currently available data and the poor inclination constraints do not allow us to confirm either hypothesis.

Despite the fact that the launch of the relativistic jet are expected to provoke significant changes in the structure of the accretion flow, only very small spectral changes are observed in the X-ray spectra in correspondence to the radio flares associated with the relativistic jets (a few per cent in the hard emission; see Motta et al. 2011). The sole dramatic changes observed (almost) simultaneously to the launch of the jets are the transitions between type-C and type-B QPOs (see e.g. Miyamoto et al. 1991; Takizawa et al. 1997). We note, however, that it has been suggested that major radio flares seen across the hard to soft transition could be produced by internal shocks associated with varying/increasing jet velocities. If this is the case, only small changes are expected in the X-ray energy spectra and PDS (see e.g. Malzac 2013).

Our results support the hypothesis that type-B QPOs are related to the relativistic jet (Fender et al. 2009), since there is no other obvious mechanism that would be stronger face-on. Therefore, our results support what has been already proposed by Fender et al. (2004, 2009): the transitions between type-C and type-B QPOs track the dramatic changes in the configuration and/or in the physical properties of the accretion flow linked to the launch of relativistic jets (but see the case of GX 339−4, 2002 outburst; in Fender et al. 2009). As the mechanism of production of type-B QPOs and the launching mechanism of the jets is still unknown, further evidences are required to confirm this statement. Finally, the fact that the noise associated with type-B QPOs seems to be inclination independent might indicate that the type-B QPOs noise is produced by yet another mechanism, which is not sensitive to inclination effects.

5 SUMMARY AND CONCLUSIONS

We have analysed a large sample of archival *RXTE* observations were we detected LFQPOs. We assumed that there are no intrinsic differences between the sources of our sample and that the presence of absorption dips in the light curve of a source corresponds to high orbital inclination. We have shown that inclination has a strong effect on the QPOs. We found that:

(i) type-C QPOs appear stronger in high-inclination sources;
(ii) type-B QPOs show the opposite behaviour, being stronger for low-inclination sources;
(iii) the noise associated with both type-C QPOs is consistent with being stronger for low-inclination sources, while the noise associated with type-B QPOs is consistent with being inclination independent.

Our results suggest that:

(i) type-C QPOs, type-B QPOs and the broad-band noise associated with type-C QPOs are geometrically/physically different phenomena;
(ii) type-C QPOs are consistent with having a geometrical origin. In particular, we find that the relativistic precession is the only mechanism that satisfies all our observational constraints and therefore is favoured by our results;
(iii) at variance with type-C QPOs, the associated broad-band noise might, instead, correspond to intrinsic brightness variability induced by fluctuations in the mass accretion rate propagating in an hot flow that emits in a non-isotropic way;
(iv) fast transition between type-C and type-B QPOs could be the best trackers in the X-rays of the relativistic ejections typical of most BH transients.

ACKNOWLEDGEMENTS

SEM acknowledges Peggy Varniere, Lucy Heil and Erik Kuulkers for useful comments and discussion on this work. SEM and MH acknowledge support from the ESA research fellowship programme and from the ESAC Faculty. SEM also acknowledges the Observatory of Rome and Brera for hospitality. TMD and PC acknowledge support from the ESAC Faculty and ESA for hospitality. TMB and SEM acknowledge support from INAF PRIN 2012-6. TMD acknowledges funding via an EU Marie Curie Intra-European Fellowship under contract no. 2011-301355. PC acknowledges support by a Marie Curie FP7-Reintegration-Grants under contract no. 2012-322259. This research has made use of data obtained from the High Energy Astrophysics Science Archive Research Center (HEASARC), provided by NASA's Goddard Space Flight Center.

REFERENCES

Altamirano D. et al., 2011, ApJ, 742, L17
Antonucci R., 1993, ARA&A, 31, 473
Armitage P. J., Livio M., 1998, ApJ, 493, 898
Bayless A. J., Robinson E. L., Hynes R. I., Ashcraft T. A., Cornell M. E., 2010, ApJ, 709, 251
Beer M. E., Podsiadlowski P., 2002, MNRAS, 331, 351
Belloni T., Hasinger G., 1990, A&A, 230, 103
Belloni T., Psaltis D., van der Klis M., 2002, ApJ, 572, 392
Belloni T., Homan J., Motta S., Ratti E., Méndez M., 2007, MNRAS, 379, 247
Belloni T. M., Sanna A., Méndez M., 2012, MNRAS, 426, 1701
Bianchi S., Maiolino R., Risaliti G., 2012, Adv. Astron., 2012, 782030
Cabanac C., Henri G., Petrucci P.-O., Malzac J., Ferreira J., Belloni T. M., 2010, MNRAS, 404, 738
Casares J., Jonker P. G., 2014, Space Sci. Rev., 183, 223
Casella P., Belloni T., Stella L., 2005, ApJ, 629, 403
Corbel S., Kaaret P., Fender R. P., Tzioumis A. K., Tomsick J. A., Orosz J. A., 2005, ApJ, 632, 504
Corral-Santana J. M., Casares J., Shahbaz T., Zurita C., Martínez-Pais I. G., Rodríguez-Gil P., 2011, MNRAS, 413, L15
Corral-Santana J. M., Casares J., Muñoz-Darias T., Rodríguez-Gil P., Shahbaz T., Torres M. A. P., Zurita C., Tyndall A. A., 2013, Science, 339, 1048
Cowley A. P., Schmidtke P. C., Hutchings J. B., Crampton D., 2002, ApJ, 123, 1741
D'Aì A., Iaria R., Di Salvo T., Riggio A., Burderi L., Robba N. R., 2014, A&A, 564, A62

Downloaded from https://academic.oup.com/mnras/article-abstract/447/2/2059/2593782 by tomaso.belloni@inaf.it on 11 May 2020

de Jong J. A., van Paradijs J., Augusteijn T., 1996, A&A, 314, 484
Díaz Trigo M., Parmar A. N., Boirin L., Motch C., Talavera A., Balman S., 2009, A&A, 493, 145
Esin A. A., McClintock J. E., Narayan R., 1997, ApJ, 489, 865
Fender R., Belloni T., 2004, ARA&A, 42, 317
Fender R. P., Belloni T. M., Gallo E., 2004, MNRAS, 355, 1105
Fender R. P., Homan J., Belloni T. M., 2009, MNRAS, 396, 1370
Filippenko A. V., Chornock R., 2001, IAU Circ., 7644, 2
Foulkes S. B., Haswell C. A., Murray J. R., 2010, MNRAS, 401, 1275
Frank J., King A. R., Lasota J.-P., 1987, A&A, 178, 137
Gallo E., Fender R. P., Pooley G. G., 2003, MNRAS, 344, 60
Galloway D. K., 2012, Astrono. Telegram, 4014, 1
Gierliński M., Zdziarski A. A., 2005, MNRAS, 363, 1349
Gierliński M., Middleton M., Ward M., Done C., 2008, Nature, 455, 369
Greene J., Bailyn C. D., Orosz J. A., 2001, ApJ, 554, 1290
Heil L. M., Uttley P., Klein-Wolt M., 2014, preprint (arXiv:e-prints)
Hjellming R. M., Rupen M. P., Mioduszewski A. J., Smith D. A., Harmon B. A., Waltman E. B., Ghigo F. D., Pooley G. G., 1998a, BAAS, 30, 1405
Hjellming R. M. et al., 1998b, IAU Circ., 6937, 1
Homan J., Wijnands R., van der Klis M., Belloni T., van Paradijs J., Klein-Wolt M., Fender R., Méndez M., 2001, ApJS, 132, 377
Homan J., van der Klis M., Jonker P. G., Wijnands R., Kuulkers E., Méndez M., Lewin W. H. G., 2002, ApJ, 568, 878
Homan J., Miller J. M., Wijnands R., van der Klis M., Belloni T., Steeghs D., Lewin W. H. G., 2005a, ApJ, 623, 383
Homan J., Buxton M., Markoff S., Bailyn C. D., Nespoli E., Belloni T., 2005b, ApJ, 624, 295
Ingram A., Done C., 2011, MNRAS, 415, 2323
Ingram A., Done C., 2012, MNRAS, 419, 2369
Ingram A., van der Klis M., 2013, MNRAS, 434, 1476
Ingram A., Done C., Fragile P. C., 2009, MNRAS, 397, L101
Kaluzienski L. J., Holt S. S., 1977, IAU Circ., 3099, 1
Kennea J. A., Krimm H., Mangano V., Curran P., Romano P., Evans P., Burrows D. N., 2010, Astron. Telegram, 2877, 1
Kotani T. et al., 2000, ApJ, 543, L133
Kuulkers E., Parmar A. N., Kitamoto S., Cominsky L. R., Sood R. K., 1997, MNRAS, 291, 81
Kuulkers E., Wijnands R., Belloni T., Mendez M., van der Klis M., van Paradijs J., 1998, ApJ, 494, 753
Kuulkers E. et al., 2000, A&A, 358, 993
Kuulkers E. et al., 2010, Astron. Telegram, 2912, 1
Kuulkers E. et al., 2013, A&A, 552, A32
Lamb F. K., Miller M. C., 2001, ApJ, 554, 1210
Leahy D. A., Elsner R. F., Weisskopf M. C., 1983, ApJ, 272, 256
McClintock J. E., Remillard R. A., Rupen M. P., Torres M. A. P., Steeghs D., Levine A. M., Orosz J. A., 2009, ApJ, 698, 1398
Malzac J., 2013, MNRAS, 429, L20
Mann H. B., Whitney D. R., 1947, Ann. Math. Stat., 18, 50
Markert T. H., Canizares C. R., Clark G. W., Lewin W. H. G., Schnopper H. W., Sprott G. F., 1973, ApJ, 184, L67
Markwardt C. B., Swank J. H., 2003, Astron. Telegram, 133, 1
Markwardt C. B. et al., 2009a, Astron. Telegram, 2258, 1
Markwardt C. B., Barthelmy S. D., Evans P. A., Swank J. H., 2009b, Astron. Telegram, 2261, 1
Matilsky T. A., Giacconi R., Gursky H., Kellogg E. M., Tananbaum H. D., 1972, ApJ, 174, L53
Middleton M., Done C., 2010, MNRAS, 403, 9
Miller J. M. et al., 2006, ApJ, 646, 394
Miller-Jones J. C. A., Jonker P. G., Ratti E. M., Torres M. A. P., Brocksopp C., Yang J., Morrell N. I., 2011, MNRAS, 415, 306
Miller-Jones J. C. A. et al., 2012, MNRAS, 421, 468
Miyamoto S., Kitamoto S., 1991, ApJ, 374, 741
Miyamoto S., Kimura K., Kitamoto S., Dotani T., Ebisawa K., 1991, ApJ, 383, 784
Motch C., Ricketts M. J., Page C. G., Ilovaisky S. A., Chevalier C., 1983, A&A, 119, 171
Motta S., Muñoz-Darias T., Casella P., Belloni T., Homan J., 2011, MNRAS, 418, 2292
Motta S., Homan J., Muñoz Darias T., Casella P., Belloni T. M., Hiemstra B., Méndez M., 2012, MNRAS, 427, 595
Motta S. E., Muñoz-Darias T., Sanna A., Fender R., Belloni T., Stella L., 2014a, MNRAS, 439, 65
Motta S. E., Belloni T. M., Stella L., Muñoz-Darias T., Fender R., 2014b, MNRAS, 437, 2554
Muñoz-Darias T., Casares J., Martínez-Pais I. G., 2008, MNRAS, 385, 2205
Muñoz-Darias T., Motta S., Pawar D., Belloni T. M., Campana S., Bhattacharya D., 2010, MNRAS, 404, L94
Muñoz-Darias T., Coriat M., Plant D. S., Ponti G., Fender R. P., Dunn R. J. H., 2013, MNRAS, 432, 1330
Negoro H. et al., 2010, Astron. Telegram, 2873, 1
Nespoli E., Belloni T., Homan J., Miller J. M., Lewin W. H. G., Méndez M., van der Klis M., 2003, A&A, 412, 235
Neustroev V. V., Veledina A., Poutanen J., Zharikov S. V., Tsygankov S. S., Sjoberg G., Kajava J. J. E., 2014, MNRAS, 445, 2424
Orosz J. A., Remillard R. A., Bailyn C. D., McClintock J. E., 1997, ApJ, 478, L83
Orosz J. A., Jain R. K., Bailyn C. D., McClintock J. E., Remillard R. A., 1998, ApJ, 499, 375
Orosz J. A. et al., 2002, ApJ, 568, 845
Orosz J. A., McClintock J. E., Remillard R. A., Corbel S., 2004, ApJ, 616, 376
Orosz J. A., Steiner J. F., McClintock J. E., Torres M. A. P., Remillard R. A., Bailyn C. D., Miller J. M., 2011, ApJ, 730, 75
Palmer D. M., Barthelmey S. D., Cummings J. R., Gehrels N., Krimm H. A., Markwardt C. B., Sakamoto T., Tueller J., 2005, Astron Telegram, 546, 1
Parmar A. N., White N. E., 1988, in Pallavicini R., White N. E., eds, X-ray Astronomy with EXOSAT. Consiglio Nazionale delle Ricerche, Societa Astronomica Italiana, Roma, p. 147
Parmar A. N., Oosterbroek T., Boirin L., Lumb D., 2002, A&A, 386, 910
Patterson J., Robinson E. L., Nather R. E., 1977, ApJ, 214, 144
Ponti G., Fender R. P., Begelman M. C., Dunn R. J. H., Neilsen J., Coriat M., 2012, MNRAS, 422, L11
Poutanen J., Krolik J. H., Ryde F., 1997, MNRAS, 292, L21
R Development Core Team 2011, R: A Language and Environment for Statistical Computing. R Foundation for Statistical Computing. Vienna
Remillard R., 2001, IAU Circ., 7707, 1
Remillard R. A., Muno M. P., McClintock J. E., Orosz J. A., 2002, ApJ, 580, 1030
Revnivtsev M. G., Trudolyubov S. P., Borozdin K. N., 2000, MNRAS, 312, 151
Revnivtsev M., Chernyakova M., Capitanio F., Westergaard N. J., Shoenfelder V., Gehrels N., Winkler C., 2003, Astron. Telegram, 132, 1
Risaliti G., Elvis M., Nicastro F., 2002, ApJ, 571, 234
Robinson E. L., Welsh W. F., Young P., 2001, in Nicholas E. W., Giuseppe M., Giorgio G.C., eds, AIP Conf. Proc. Vol. 599, X-ray Astronomy: Stellar Endpoints, AGN, and the Diffuse X-ray Background. Am. Inst. Phys., New York, p. 902
Rupen M. P., Hjellming R. M., Mioduszewski A. J., 1998, IAU Circ., 6938, 2
Schnittman J. D., Homan J., Miller J. M., 2006, ApJ, 642, 420
Shahbaz T., van der Hooft F., Casares J., Charles P. A., van Paradijs J., 1999, MNRAS, 306, 89
Shakura N. I., Sunyaev R. A., 1973, A&A, 24, 337
Smale A. P., Wachter S., 1999, ApJ, 527, 341
Smith D. A., 1998, IAU Circ., 7008, 1
Smith D. A., Levine A., Wood A., 1998, IAU Circ., 6932, 1
Soleri P., Fender R., 2011, MNRAS, 413, 2269
Soleri P., Belloni T., Casella P., 2008, MNRAS, 383, 1089
Soleri P. et al., 2013, MNRAS, 429, 1244
Steiner J. F. et al., 2012a, MNRAS, 427, 2552
Steiner J. F., McClintock J. E., Reid M. J., 2012b, ApJ, 745, L7
Stella L., Vietri M., 1999, Phys. Rev. Lett., 82, 17

Downloaded from https://academic.oup.com/mnras/article-abstract/447/2/2059/2593782 by tomaso.belloni@inaf.it on 11 May 2020

Stiele H., Motta S., Muñoz-Darias T., Belloni T. M., 2011, MNRAS, 418, 1746
Strohmayer T. E., Mushotzky R. F., 2003, ApJ, 586, L61
Tagger M., Pellat R., 1999, A&A, 349, 1003
Takizawa M. et al., 1997, ApJ, 489, 272
Titarchuk L., Fiorito R., 2004, ApJ, 612, 988
Titarchuk L., Osherovich V., 1999, ApJ, 518, L95
Tomsick J. A., Lapshov I., Kaaret P., 1998, ApJ, 494, 747
Urry C. M., Padovani P., 1995, PASP, 107, 803
van der Hooft F., Heemskerk M. H. M., Alberts F., van Paradijs J., 1998, A&A, 329, 538
van der Klis M., 1989, ARA&A, 27, 517
Varnière P., Blackman E. G., 2005, New Astron., 11, 43
Varnière P., Tagger M., 2002, A&A, 394, 329
Varnière P., Tagger M., Rodriguez J., 2012, A&A, 545, A40
Veledina A., Poutanen J., Ingram A., 2013, ApJ, 778, 165
Walter F. M., Mason K. O., Clarke J. T., Halpern J., Grindlay J. E., Bowyer S., Henry J. P., 1982, ApJ, 253, L67
White N. E., Holt S. S., 1982, ApJ, 257, 318
White N. E., Mason K. O., 1985, Space Sci. Rev., 40, 167
White N. E., Swank J. H., 1982, ApJ, 253, L61
Wijnands R., Homan J., van der Klis M., 1999, ApJ, 526, L33
Wijnands R., Miller J. M., Lewin W. H. G., 2001, IAU Circ., 7715, 2
Wood A., Smith D. A., Marshall F. E., Swank J., 1999, IAU Circ., 7274, 1
Zhang S. N., Wilson C. A., Harmon B. A., Fishman G. J., Wilson R. B., Paciesas W. S., Scott M., Rubin B. C., 1994, IAU Circ., 6046, 1
Zhang W., Jahoda K., Swank J. H., Morgan E. H., Giles A. B., 1995, ApJ, 449, 930

APPENDIX A: ON THE RELATION BETWEEN HIGH INCLINATION AND ABSORPTION DIPS

Absorption dips in the X-ray light curves usually recur at the orbital period of a system and are thought to be caused by obscuration by material located in a thickened outer region ('bulge') of the accretion disc. The bulge forms as a consequence of the interaction of the accretion disc with the inflowing gas stream from the companion star (see e.g. Walter et al. 1982; White & Swank 1982). The presence of absorption dips is commonly considered a signature of high orbital inclination (but see Galloway 2012)[9] and can allow measurement of the orbital period of a source (White & Swank 1982; White & Mason 1985; Díaz Trigo et al. 2009; Casares & Jonker 2014). Absorption dips in low-mass X-ray binaries (LMXBs) have been observed mainly around orbital phase 0.7–0.9, while eclipses are expected at phase zero when the accretion disc is seen at $\sim 90^\circ$, i.e. when the companion star is closest to us and in front of the compact object (e.g. Parmar & White 1988). Occasionally, 'secondary absorption dips' are observed at a 0.5 phase difference with respect to the phase at which 'regular dips' occur are also observed. They are explained as being due to material migrating to the other side after the impact with the disc (see e.g. Frank, King & Lasota 1987; Armitage & Livio 1998, and references therein).

The orbital inclination angle with respect to the line of sight necessary to produce absorption dips depends both on the geometry of the system and on the properties of the accretion flow (e.g. the size of the accretion disc and of the bulge) and therefore might be different for every source. However, it is still possible to estimate the minimum inclination angle that would provoke absorption dips in a standard BHB. This lower limit on the inclination is based on the size of the bulge and not on the disc opening angle, which has been generally estimated to be $\simeq 12^\circ$ (e.g. de Jong, van Paradijs & Augusteijn 1996; Bayless et al. 2010). White & Holt (1982) estimated the size of the bulge responsible for absorption dips as $19^\circ \pm 6^\circ$ for the LMXB 4U 1822−37. Taking this value as typical for LMXBs, we can thus set a lower limit on the disc inclination of 65°. We note, however, that if the accretion disc is tilted or warped, the lower limit for the inclination could be as low as 55°, by considering that for a generic LMXBs, a disc tilt of about 10° is expected (Foulkes, Haswell & Murray 2010).

In several LMXBs the absorption dips appear for only part of the outburst (see e.g. in MAXI J1659−152, Kuulkers et al. 2013; 4U 1630−47 and GRO J1655−40, Kuulkers et al. 1998, 2000; Tomsick et al. 1998; H1743−322, Homan et al. 2005b). The explanation for this lies on the fact that for transient BHXBs, changes in the accretion mode cause the appearance or disappearance of dips. For instance, Kuulkers et al. (2000) interpreted the (deep) absorption dips during the rise and plateau phase of the outburst in GRO J1655−40 as due to filaments in the stream of material coming from the companion star and splashing into the accretion disc, overflowing above and below the impact region. If the inclination is high enough, the impact region itself comes also into the line of sight (e.g. Frank et al. 1987). However, the presence of absorption features all around the orbit for NS (e.g. Parmar et al. 2002) shows that at least part of the photoionized plasma is distributed equatorially along the whole plane of the disc, indicating that absorption is due to a structure in the disc rather than by filaments. In that scenario, the cause for the disappearance of dips in BHXBs could be, e.g. a strong ionization of the plasma in bright (but hard) states of the outburst, which renders the plasma transparent and therefore invisible to the observer. An alternative explanation could be that a change of the structure of the accretion flow could diminish the thickness of the bulge and cause the absorption dips to disappear.

APPENDIX B: ON THE INCLINATION OF THE SOURCES OF OUR SAMPLE

The inclination angle of a binary with respect to the line of sight can be obtained, in absence of eclipses, through indirect methods based on information from the light curve and the spectrum of the optical companion star. The binary inclination is commonly obtained through fitting optical/NIR (near-infrared) light curves with synthetic ellipsoidal models, since the amplitude of the modulation normally observed in the OIR light curves strongly depends on the inclination angle. However, the vast majority of transient XRBs posses a faint K–M donor star and therefore their light curves can be seriously contaminated by other non-stellar sources of light (e.g. the outer accretion disc), affecting critically the inclination measurement.

B1 Swift J1753.5−0127

SWIFT J1753.5−0127 is an X-ray transient discovered by the *Swift*/BAT on 2005 as a bright variable X-ray source (Palmer et al. 2005). Although the mass of the primary has not been dynamically measured yet, the system displayed a number of characteristics that suggest that the binary hosts a BH (Soleri et al. 2013).

Neustroev et al. (2014) reported results from optical and UV observations of Swift J1753.5−01. Despite the fact that very low values for inclination are to be excluded (e.g. no absorption

[9] Galloway (2012) reported apparent dipping activity early in the 2011 outburst of the NS XRB Aql X-1. Such features had not been previously reported in Aql X-1, but resembled the absorption dips observed in other XRBs. Galloway (2012) therefore concluded that, since apparent dipping behaviour can occur at times, the system inclination is at the high end of its likely range (36°–55°), Robinson, Welsh & Young (2001).

Downloaded from https://academic.oup.com/mnras/article-abstract/447/2/2059/2593782 by tomaso.belloni@inaf.it on 11 May 2020

lines – typical of high-inclination bright X-ray novae – and orbital-like modulation in the light curve that suggest inclination larger than 40°), high orbital inclination values must be also excluded for two reasons. First, extensive photometry and spectroscopy of Swift J1753.5−01 rule out any significant absorption dip or eclipse, commonly considered a signature of high inclination. Secondly, given the orbital parameters of Swift J1753.5−01, inclinations larger than ∼55° are highly improbable, since it would require a physically unacceptable BH mass smaller than ∼2 $M_{\odot}$.

B2 4U 1543−47

4U 1543−47 is a bright soft X-ray transient, first observed in outburts in 1971 (Matilsky et al. 1972). Based on its spectral properties, the compact object has been classified as a BH candidate.

The presence of (small) ellipsoidal modulations in the optical light curve of the source allowed Orosz et al. (1998) to constrain the inclination between 24° and 36° (obtained fitting the *V* and *I* optical light curves), with extreme hard lower and upper limits at 20° and 40°, respectively. The second set of limits takes into account possible systematics that the ellipsoidal modelling does not account for.

B3 XTE J1650−500

XTE J1650−500 was discovered by *RXTE* in 2001 (Remillard 2001) and classified as a strong BH candidate based on its X-ray spectrum and variability properties (see e.g. Wijnands, Miller & Lewin 2001).

Orosz et al. (2004) performed a photometric and spectroscopic analysis of XTE J1650−500, and reported a lower limit to the orbital inclination of ∼47°, assuming no disc contamination of the optical light curve. Because of lack of eclipses, Orosz et al. (2004) concluded that the inclination must be lower than ∼70°, even though the exact value depends on the mass ratio on the binary. However, these authors noted that to obtain an inclination of ∼70° the accretion disc should contribute 80 per cent of the optical emission. Additionally, Orosz et al. (2004) showed that an inclination higher than 70° would yield a BH mass lower than 4 $M_{\odot}$.

B4 GX 339−4

GX 339−4 was discovered by OSO 7 in 1972 (Markert et al. 1973). Even when GX 339−4 was first discovered, its aperiodic X-ray variability on time-scales from milliseconds to seconds suggested that the compact object in the system is a BH. This transient source is among the most studied by *RXTE*, having shown four outbursts in the last decade.

Cowley et al. (2002) reported the results from simultaneous optical photometric and spectroscopic observations. Only small amplitudes in the emission-line velocity were visible, suggesting that GX 339−4 is seen at a low orbital inclination angle. This is confirmed by the lack of eclipses and absorption dips in both the optical and X-ray light curves (Muñoz-Darias et al. 2008), which allow us to set an upper limit on the inclination of ∼70°. However, a lower limit to the inclination can be set assuming that the BH mass should not exceed 20 $M_{\odot}$: under this hypothesis, the large estimate of the mass function for GX 339−4 implies an inclination larger than 40°.

B5 XTE J1752−223

XTE J1752−223 was discovered on 2009 October 23 by *RXTE* (Markwardt et al. 2009a). The properties of the X-ray spectrum and the lack of pulsations in the X-ray band suggested that the source was a BH candidate (Markwardt et al. 2009b), conclusion supported by Muñoz-Darias et al. (2010).

Since XTE J1752−223 has not shown absorption dips nor eclipses, we can assume an upper limit on the inclination of ∼70°. Miller-Jones et al. (2011) reported the detection of compact radio emission from the core of XTE J1752−223, which can be associated with the relativistic ejections from the source. Assuming the radio jet as perpendicular to the orbital plane, the inclination of XTE J1752−223 must be lower than ∼49°.

B6 XTE J1859+226

XTE J1859+226 was discovered during its 1999 outburst (Wood et al. 1999) and its X-ray properties allowed us to classify it as a BH candidate. Corral-Santana et al. (2011) performed photometry of the source and found a mass function significantly smaller than the ones previously estimated (see e.g. Filippenko & Chornock 2001), but still consistent with the presence of a BH.

The lack of eclipses allowed Corral-Santana et al. (2011) to set an upper limit to the source inclination to 70°. Assuming no contribution from the accretion disc to the optical emission, an inclination of at least 60° is needed to reproduce the large modulations observed in the light curve. A disc contribution to the optical light curve equal to 25 per cent would result in an inclination angle of ∼70°. This suggests that XTE J1859+226 might be at intermediate inclination with respect to the line of sight. This is confirmed by the spectral properties of the source. Despite the lack of clear absorption dips, Muñoz-Darias et al. (2013) noted that XTE J1859+27 showed the characteristic flux spikes in its HIDs and light curves, typical of high-inclination sources.

B7 XTE J1550−564

XTE J1550−564 was discovered on 1998 (Smith 1998) by *RXTE*. Orosz et al. (2011) performed moderate-resolution optical spectroscopy and NIR photometry of the source and were able to determine the mass function for the binary system. Orosz et al. (2011) fitted the light curves from different wavebands obtained over a 8 yr of observations (2001–2009) with a number of models, combining different subsets of data and assuming variable disc-contributions to the optical emission and obtaining different values for the orbital inclination. Although the fit to the light curve from a small subset of data (collected in 2006–2007) yielded an inclination of ∼57°, the best fit to the overall optical data (considered more reliable by the authors) corresponds to an inclination of (74.69 ± 3.8)°.

B8 4U 1630−47

4U 1630−47 has shown outbursts every ∼600 d since at least 1969 (Kuulkers et al. 1997). Even if the nature of the compact object is still to be confirmed, the X-ray spectral and timing properties of 4U 1630−47 point to a BH.

Kuulkers et al. (1998) discovered absorption dips of a typical duration of a few minutes in the X-ray light curve of 4U 1630−47, but no eclipses, which allowed these authors to constrain the inclination of the source between 65° and 75°. The lack of other significant information does not allow us to place any other constraints on the source inclination.

Downloaded from https://academic.oup.com/mnras/article-abstract/447/2/2059/2593782 by tomaso.belloni@inaf.it on 11 May 2020

B9 GRO J1655−40

GRO J1655−40 was discovered in 1994 by the *Compton Gamma-Ray Observatory* (Zhang et al. 1994). Since this system has a relatively luminous F companion star, the quiescent light curve is dominated by star light at an unusual extent and, as a result, an unusually precise determination of the orbital parameters is possible.

Orosz et al. (1997) reported a first inclination measurement of 69.50 ± 0.08. Later works, based on larger data sets, reported refined inclination measurements, all within the 63°–75° range (van der Hooft et al. 1998; Shahbaz et al. 1999). Greene et al. (2001) performed multiwavelength photometry of GRO J1655−40, obtaining an inclination of $(70.2 \pm 1.9)^\circ$. The most recent fit to the multiwavelength light curve of GRO J1655−40 is reported in Beer & Podsiadlowski (2002), which obtained an inclination of $(68.65 \pm 1.5)^\circ$.

B10 H1743−322

First detected during an outburst in 1977 (Kaluzienski & Holt 1977), H1743−322 was rediscovered as a new source in 2003 by *INTEGRAL* (Revnivtsev et al. 2003) and only subsequently associated with the previously known source (Markwardt & Swank 2003). Since that time, several smaller outbursts of the source have been observed. From its similarities with the dynamically confirmed BH XTE J1550−564, H1743−322 was classified as a BH candidate (see McClintock et al. 2009), although no mass function has yet been reported.

Homan et al. (2005a) and Miller et al. (2006) reported observations of absorption dips from this source, appeared only after years of monitoring of the source. This indicates that the orbital inclination is relatively high, possibly on the order of ∼80°. Steiner, McClintock & Reid (2012b) determined the inclination of the radio jet with respect to the line of sight to be $(75 \pm 3)^\circ$, which confirms the high inclination of the source if we assume that the disc and the jet axes are (almost) aligned.

B11 MAXI J1659−152

MAXI J1659−152 was discovered in 2010 September by *Swift*/BAT. The source was initially designated as a gamma-ray burst and subsequently classified as an X-ray transient thanks to MAXI data (Negoro et al. 2010).

Kennea et al. (2010) reported frequent intensity drops in the X-ray light curve, possibly attributed to absorption dips or partial eclipses. Kuulkers et al. (2010, 2013) confirmed the detection of absorption dips and established an orbital period of ∼2.42 h for the source. The presence of the absorption dips also allowed these authors to constrain the inclination of the orbital plane of MAXI J1659−152 between 65° and 80°.

B12 MAXI J1543−564

MAXI J1543−564 was discovered by MAXI in 2011. The spectral and timing properties of the sources allowed us to classify the compact object in the system as a BH candidate (Stiele et al. 2011).

No mass function has been reported for this source and no information is available to allow us to measure or constrain the inclination of this source. Hints pointing to intermediate inclination can be found in the typical spikes that can be observed in the HID and light curve of the system, reported by Stiele et al. (2011) and discussed by Muñoz-Darias et al. (2013). However, since no absorption dips nor eclipses have been observed (yet), it is not possible to further constrain the inclination of the source.

B13 XTE J1748−288

XTE J1748−288 was discovered on 1998 by the *RXTE*/ASM (Smith, Levine & Wood 1998). An optically thin radio counterpart was discovered by Hjellming et al. (1998b) and subsequently the source was resolved by VLA (Rupen, Hjellming & Mioduszewski 1998). Follow up observations confirmed the detection of a radio jet, making XTE J1748−288 one of the few sources displaying apparent superluminal motion (Hjellming et al. 1998a).

Revnivtsev, Trudolyubov & Borozdin (2000) reported a sharp dip in the 1530-keV emission in the *RXTE*/PCA data, while Kotani et al. (2000) derived an inclination of the jet of $<70^\circ$ from proper motion. These information suggest that XTE J1748−288 is seen at high inclination, even though the absorption nature of the dips observed by Revnivtsev et al. (2000) is to be confirmed.

SUPPORTING INFORMATION

Additional Supporting Information may be found in the online version of this article:

Table 2. QPO, noise and total rms from all the observations on the sources of our sample (http://mnras.oxfordjournals.org/lookup/suppl/doi:10.1093/mnras/stu2579/-/DC1).

Please note: Oxford University Press are not responsible for the content or functionality of any supporting materials supplied by the authors. Any queries (other than missing material) should be directed to the corresponding author for the article.

This paper has been typeset from a TEX/LATEX file prepared by the author.

Downloaded from https://academic.oup.com/mnras/article-abstract/447/2/2059/2593782 by tomaso.belloni@inaf.it on 11 May 2020